SCIENTIFIC REPORTS

OPEN

SUBJECT AREAS:
REGENERATION
PERIPHERAL VASCULAR DISEASE
ANGIOGENESIS
TISSUE ENGINEERING AND REGENERATIVE MEDICINE

Received
6 September 2012

Accepted
25 February 2013

Published
11 March 2013

Correspondence and requests for materials should be addressed to R.S. (rshibata@med.nagoya-u.ac.jp) or T.M. (murohara@med.nagoya-u.ac.jp)

iPS cell sheets created by a novel magnetite tissue engineering method for reparative angiogenesis

Tetsutaro Kito[1], Rei Shibata[1], Masakazu Ishii[1], Hirohiko Suzuki[1], Tatsuhito Himeno[2], Yoshiyuki Kataoka[1], Yumiko Yamamura[1], Takashi Yamamoto[1], Naomi Nishio[2], Sachiko Ito[2], Yasushi Numaguchi[1], Tohru Tanigawa[3], Jun K. Yamashita[4], Noriyuki Ouchi[5], Hiroyuki Honda[6], Kenichi Isobe[2] & Toyoaki Murohara[1]

[1]Department of Cardiology, Nagoya University Graduate School of Medicine, [2]Department of Immunology, Nagoya University Graduate School of Medicine, [3]Department of Otolaryngology, Aichi Medical University, [4]Department of Stem Cell Differentiation, Institute for Frontier Medical Sciences, Kyoto University, [5]Department of Molecular Cardiology, Nagoya University Graduate School of Medicine, [6]Department of Biotechnology, Nagoya University Graduate School of Engineering.

Angiogenic cell therapy represents a novel strategy for ischemic diseases, but some patients show poor responses. We investigated the therapeutic potential of an induced pluripotent stem (iPS) cell sheet created by a novel magnetite tissue engineering technology (Mag-TE) for reparative angiogenesis. Mouse iPS cell-derived Flk-1$^+$ cells were incubated with magnetic nanoparticle-containing liposomes (MCLs). MCL-labeled Flk-1$^+$ cells were mixed with diluted extracellular matrix (ECM) precursor and a magnet was placed on the reverse side. Magnetized Flk-1$^+$ cells formed multi-layered cell sheets according to magnetic force. Implantation of the Flk-1$^+$ cell sheet accelerated revascularization of ischemic hindlimbs relative to the contralateral limbs in nude mice as measured by laser Doppler blood flow and capillary density analyses. The Flk-1$^+$ cell sheet also increased the expressions of VEGF and bFGF in ischemic tissue. iPS cell-derived Flk-1$^+$ cell sheets created by this novel Mag-TE method represent a promising new modality for therapeutic angiogenesis.

Therapeutic angiogenesis, a novel strategy for treating patients with severe peripheral arterial disease (PAD), promotes the formation of collateral vessels. Recently, clinical trials have confirmed the safety and efficiency of transplantation of progenitor cells derived from bone marrow or circulating blood in patients with PAD or myocardial infarction[1–5]. However, patients with severe PAD associated with multiple coronary risk factors have responded poorly to these therapies[6–8].

Induced pluripotent stem (iPS) cells were generated from mouse skin fibroblasts by introducing four transcriptional factors[9]. iPS cells could be used repeatedly and were capable of differentiating into a variety of cell types as needed. Various cardiovascular cells are directionally induced from mouse and human iPS cell-derived fetal liver kinase-1 positive (Flk-1$^+$) cells *in vitro*[10,11]. We previously demonstrated direct local implantation of mouse iPS cell-derived Flk-1$^+$ cells to augment ischemia-induced angiogenesis in a mouse model of hindlimb ischemia[12]. Thus, we speculated that iPS cell-derived Flk-1$^+$ cells might be applicable to therapeutic angiogenesis.

The most common method of cell transplantation is direct injections of cell suspensions using a needle. This simple method has several disadvantages including rapid cell loss caused by leakage of the injected suspensions, late cell loss due to unstable cell homing, and needle-mediated direct tissue damage[13–17]. Therefore, alternative cell application strategies are needed.

The cell sheet technique has advantages such as being less invasive for host muscle, rather than skin, because the cell sheet is only placed on muscle tissues. Recently, we reported a novel tissue engineering (TE) strategy, termed the magnetic force-based TE (Mag-TE) system[18–21]. We succeeded in creating a mesenchymal stem cell (MSC) sheet, comprised of 10–15 layers of cells, with an approximately 300 μm thickness. The transplanted MSC sheet was successfully engrafted into ischemic tissues of mice, and stimulated neovascularization in response to limb ischemia[21]. However, thick constructs may pose the risk of inducing ischemia of inner cell layers, due to insufficient oxygen and nutrient supplies.

In the present study, we attempted to construct multi-layered 3-D iPS cell-derived Flk-1$^+$ cell sheets combining the Mag-TE system with an ECM (extracellular matrix) precursor embedding system. We tested

the therapeutic potential of iPS cell-derived Flk-1$^+$ cell sheets for ischemia-induced angiogenesis *in vivo* using a murine model of hindlimb ischemia.

Results

Differentiation of iPS cell-derived Flk-1$^+$ cells with MCLs into vascular cells. We used the mouse iPS cell line "iPS-MEF-Ng-20D-17" generated from mouse embryonic fibroblasts by introducing four factors (Oct3/4, Sox2, Klf4 and the c-Myc mutant c-Myc T58A). First, we assessed the differentiation of iPS cell-derived Flk-1$^+$ cells magnetically labeled with nanoparticle-containing liposomes (MCLs). We induced mature endothelial cells and smooth muscle cells from Flk1$^+$ cells labeled or unlabeled with MCLs. Immunofluorescence analysis revealed that CD31$^+$ endothelial cells and α-SMA$^+$ smooth muscle cells were selectively induced from Flk1$^+$ cells, regardless of the presence or absence of labeling with MCLs (Supplementary figure 1A). There were no significant differences in the proportions of CD31$^+$ and α-SMA$^+$ cells between Flk1$^+$ cells labeled with MCLs and unlabeled Flk1$^+$ cells (Supplementary figure 1B and C). Thus, the incorporation of magnetic particles within the cells did not alter their phenotypes.

Construction of Flk-1$^+$ cell sheets by combining Mag-TE and ECM precursor embedding systems. Mouse iPS cell-derived Flk-1$^+$

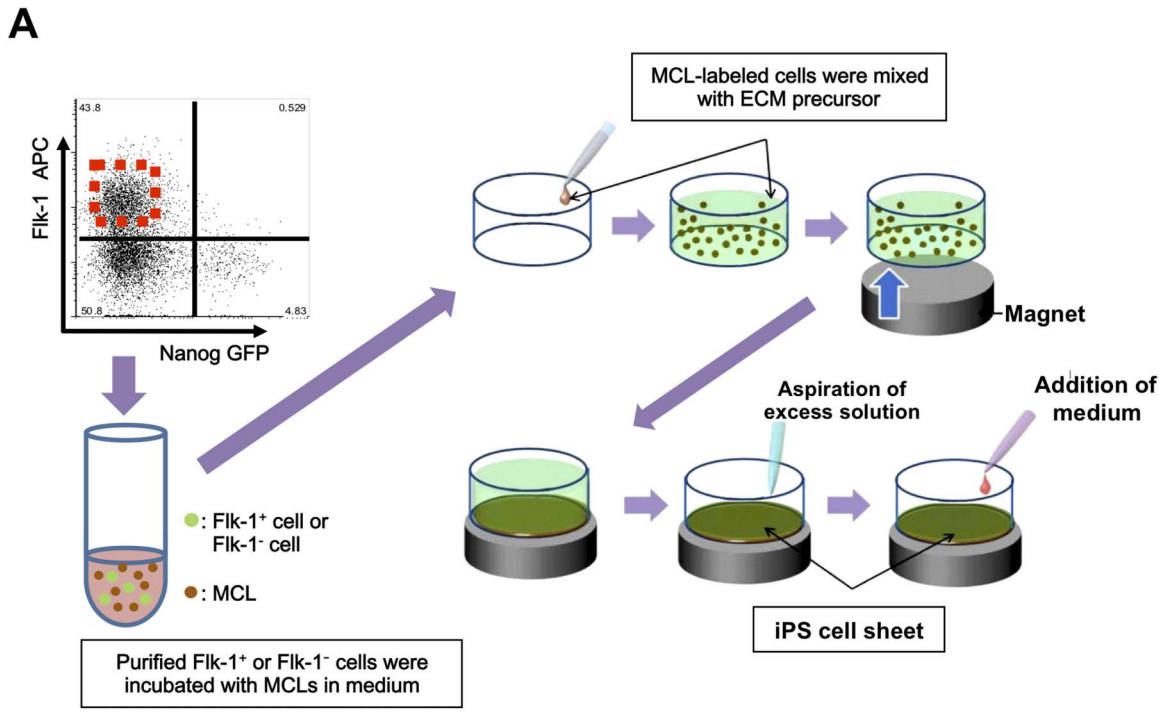

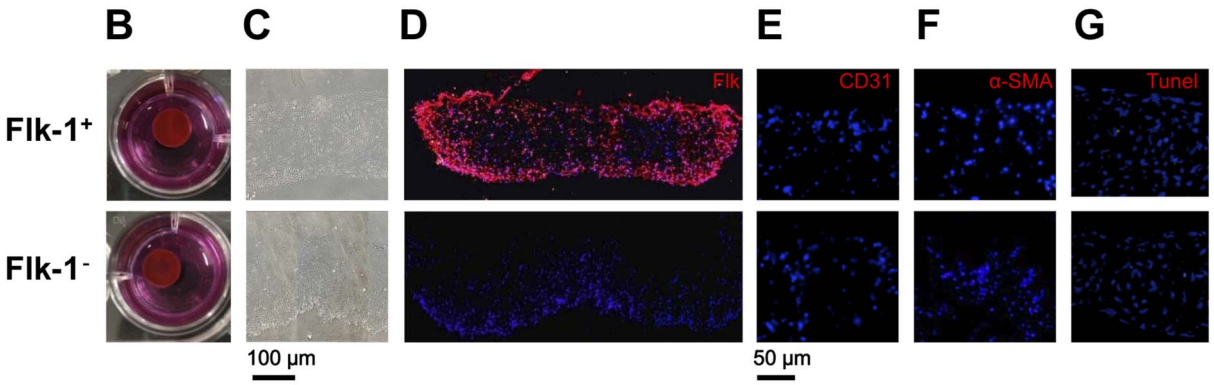

Figure 1 | Construction of iPS cell-derived cell sheet by combining Mag-TE and ECM precursor embedding systems. (A) Procedure for construction of iPS cell-derived cell sheet. After FACS sorting, floating purified cells were mixed with MCL particles and incubated for 2 hours. One × 10^6 MCL-labeled cells were mixed with ECM precursor and seeded onto ultra-low-attachment plates, which were then placed on a cylindrical neodymium magnet. Vertical magnetic force was applied to the plate. Excess ECM precursor was aspirated, a sufficient quantity of differentiation medium was then added to the plate, and incubation was continued for an additional 24 hours. (B–G) Histological examination of iPS cell-derived Flk-1$^+$ or Flk-1$^-$ cell sheets. Upper column shows the Flk-1$^+$ cell sheet, the lower column the Flk-1$^-$ cell sheet. (B) Macroscopic photographs. (C) Microscopic photographs with bright field. Immunofluorescence staining shows the presence of Flk-1 (D), CD31 (E) and αSMA (F) in an iPS cell sheet (Flk-1 = red; cell nuclei = blue). Neither CD31 nor αSMA positive cells were detected in either cell sheet. (G) Representative photomicrographs of an iPS cell sheet stained with TUNEL. Apoptotic nuclei were identified by TUNEL staining (green), and total nuclei were identified by DAPI (blue).

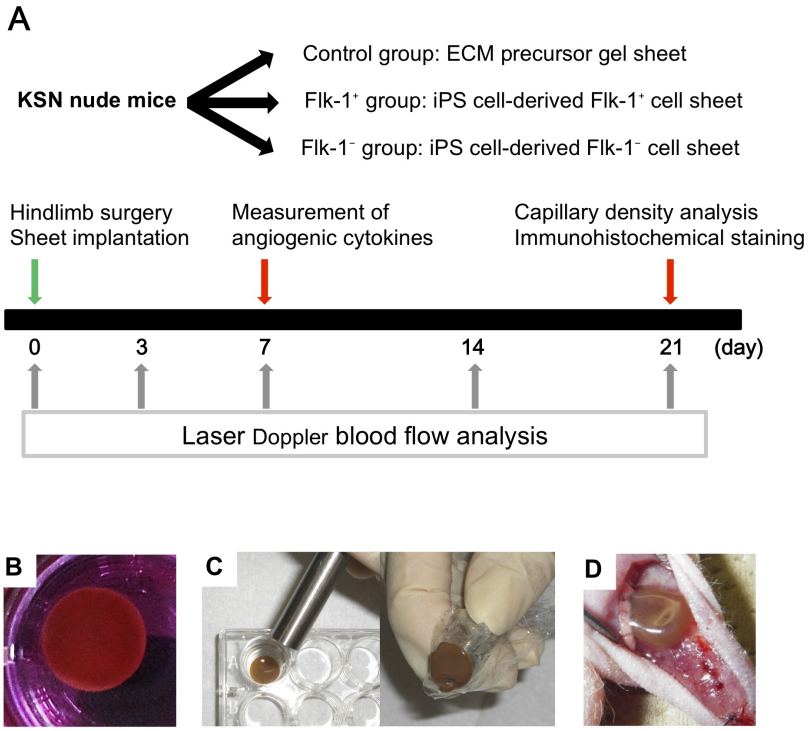

Figure 2 | Procedures for transplanting iPS cell sheets into nude mouse hindlimbs. (A) The *in vivo* experimental design. Nude mice were randomly allocated into 3 groups. The Flk-1$^+$ and Flk-1$^-$ groups received the iPS cell-derived Flk-1$^+$ and Flk-1$^-$ cell sheets, respectively, placed on ischemic adductor muscles after hindlimb surgery. The control group received the gel sheet of ECM precursors. (B) An alnico magnet was positioned on the surface of the culture medium. The Flk-1 cell sheet floated up to the surface of the culture medium without disruption. (C) The magnetized Flk-1 cell sheet attached to an Alnico magnet covered with PVDF membrane via a magnetic force. (D) Flk-1 cell sheets were placed on the adductor muscles of nude mice using the Alnico magnet.

cell sheets were constructed using the Mag-TE system and ECM precursor embedding system, in combination, as shown in Figure 1A. Figure 1B presents macroscopic views of Flk-1$^+$ or Flk-1$^-$cell sheets constructed on an ultra-low-attachment culture plate. These sheets were brown, the color of magnetite Fe_3O_4 nanoparticles, and had sufficient strength for handling. The sheet was nearly circular with a diameter of 8 millimeters. In a microscopic view, the sheets had a "reticular pattern structure" or "net-like pattern structure" comprised of pile-ups of 15 to 20 layered cells with an approximately 300 μm thickness (Figure 1C). Immunofluorescent staining confirmed the expression of Flk-1 within the Flk-1$^+$, but not the Flk-1$^-$, cell sheet (Figure 1D). CD31$^+$ endothelial cells and α-SMA$^+$ smooth muscle cells were virtually absent from these cell sheets (Figure 1E and F). Also, virtually no TUNEL positive-apoptotic cells were observed at 24 h after the initiation of sheet construction (Figure 1G). Thus, we succeeded in creating iPS cell-derived Flk-1$^+$ or Flk-1$^-$ cell sheets by combining the Mag-TE and ECM precursor embedding systems. In addition, we attempted to construct iPS cell-derived Flk-1$^+$ cell sheets from another mouse iPS cell line, BM21, generated from dendritic cells of 21-month-old C57/BL6 mice[22]. We succeeded in creating iPS cell-derived Flk-1$^+$ cell sheets from this cell line (Supplementary figure 2A and B). Our iPS cell-derived Flk-1$^+$ cell sheets combining the Mag-TE system with an ECM precursor embedding system were thus created employing two different cell lines.

Augmentation of ischemia-induced angiogenesis by iPS cell-derived Flk-1$^+$ cells sheet. We examined whether *in vivo* implantation of an iPS cell-derived Flk-1$^+$ or Flk-1$^-$ cell sheet augmented ischemia-induced angiogenesis using a mouse model of hindlimb ischemia. The assessment strategy for ischemia-induced angiogenesis *in vivo* is shown in Figure 2A. KSN athymic nude mice were randomly allocated into 3 groups. The Flk-1$^+$ and Flk-1$^-$ groups (1×10^6 cells/sheet; each group) received the iPS cell-derived Flk-1$^+$ and Flk-1$^-$ cell sheets, respectively, placed on ischemic adductor muscles after hindlimb surgery. The control group received the ECM precursor gel sheet.

Figures 2B to D show serial procedures for harvesting an iPS cell sheet created using the Mag-TE and ECM precursor embedding systems. A neodymium magnet under the culture plate was removed. Then, an Alnico magnet covered with a hydrophilic PVDF film was positioned on the surface of the culture medium. A sheet was recovered by magnetic force, and was then placed on the adductor muscles of the mouse hindlimb using the Alnico magnet. After sheet placement, the skin was closed with a simple interrupted 5-0 suture.

On gross morphologic examination at postoperative day 21, the Flk-1$^+$ and Flk-1$^-$ cell sheets showed successful engraftment, appearing as a brown spot on the ischemic tissue (Figure 3A). In the Flk-1$^+$ group, large numbers of macroscopically visible collateral blood vessels were confirmed around the sheets. No tumor formation was detected in the mice onto which Flk-1$^+$ cell sheets had been transplanted, at any time during the observation period. However, transplantation of the Flk-1$^-$ cell sheet was associated with significant rates of teratoma formation (10.8%). Therefore, *in vivo* studies were carried out after exclusion of the teratoma-forming animals.

Figure 3B shows representative laser Doppler blood flow (LDBF) images of hindlimb blood flow immediately after ischemia-inducing surgery and at different time points thereafter. Quantitative analysis revealed that the Flk-1$^+$ group showed a significant increase in limb perfusion 7, 14 and 21 days after surgery as compared to the control and Flk-1$^-$ groups (Figure 3C).

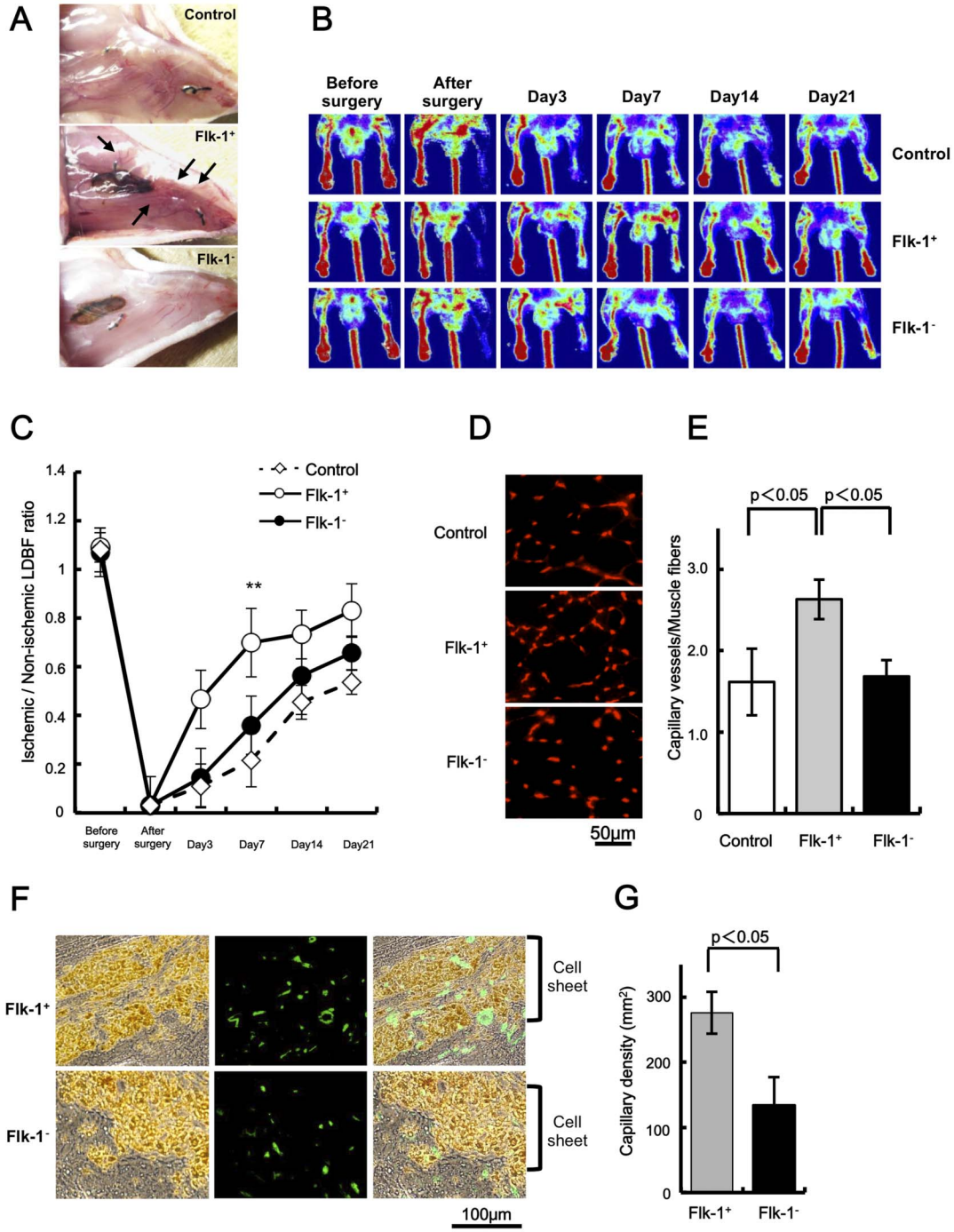

Figure 3 | Implantation of iPS cell-derived Flk-1$^+$ cell sheets augmented ischemia-induced angiogenesis. (A) Representative images of implanted cell sheets, persisting on ischemic adductor muscles on postoperative day 21. Macroscopically visible collateral blood vessels were identified around the sheets in the Flk-1$^+$ group (arrows). (B) Representative LDBF images obtained on postoperative days 3, 7, 14 and 21 (n = 5); ECM precursor gel sheet in the control (upper), Flk-1$^+$ cell sheet (middle) and Flk-1$^-$ cell sheet (lower) groups. (C) Quantitative analysis of the ischemic/normal LDBF ratio. *$p < 0.05$, * *$p < 0.001$ vs. control and Flk-1$^-$ cell sheet groups. (D) Representative photographs of capillary networks (Red = CD31) on postoperative day 21. (E) Quantitative analysis of capillary density in ischemic hindlimb tissue. (F) Representative photograph of capillary networks within and around the cell sheet (green = CD31) on postoperative day 21. (G) Quantitative analysis of capillary density within and around the cell sheet.

To investigate the extent of angiogenesis at the microcirculatory level, capillary density was measured in histological sections harvested from the ischemic adductor muscle. Representative photomicrographs of CD31-stained ischemic muscles are presented in Figure 3D. Figure 3E shows a quantitative analysis revealing that, on postoperative day 21, the tissue capillary density in ischemic muscles was significantly increased in the Flk-1$^+$ group as compared to the Flk-1$^-$ and control groups. Interestingly, capillary density within the sheet was also significantly greater in the Flk-1$^+$ than in the Flk-1$^-$ group (Figure 3F and G).

Transplantation of iPS cell-derived Flk-1$^+$ cell sheets increased VEGF and bFGF expressions. We investigated whether transplantation of iPS cell-derived Flk-1$^+$ cell sheets stimulated the expressions

of vascular endothelial growth factor (VEGF) and basic fibroblast growth factor (bFGF) in ischemic hindlimb tissues. On postoperative day 7, mouse VEGF and bFGF mRNA levels were increased in the Flk-1$^+$ group as compared to the Flk-1$^-$ and control groups (Figure 4A and B).

Transplantation of iPS cell-derived Flk-1$^+$ cell sheets promotes angiogenesis more effectively than conventional direct-injection of Flk-1$^+$ cell suspension. We assessed the effect of Flk-1$^+$ cell transplantation via a needle injection on blood flow recovery of ischemic muscle, as compared to that of transplantation of Flk-1$^+$ cell sheets. The Flk-1$^+$ cell-injected group showed a significant increase in limb blood perfusion on days 3, 7, 14 and 21 after surgery as compared to the phosphate buffered saline (PBS)-injected group (Figure 5A). Blood perfusion was greater in the ischemic limbs of the Flk-1$^+$ cell-sheet group than in those of the Flk-1$^+$ cell-injected group (Figure 5A).

We also created iPS cell-derived Flk-1$^+$ cell sheets using only the ECM precursor embedding system, and assessed the effect of this sheet on blood flow recovery of ischemic muscle. The iPS cell-derived Flk-1$^+$ cell sheet created employing only the ECM precursor embedding system suffered from fluctuations in cellular density and did not have an adequate sheet-like structure (Supplementary figure 3A and B). Implantation of iPS cell-derived Flk-1$^+$ cell sheets created employing only the ECM precursor embedding system (the Flk-1$^+$ cell-ECM group) did not achieve increased recovery of blood flow as compared to the PBS-injected group (Figure 5A).

Furthermore, VEGF and bFGF mRNA levels were increased in the Flk-1$^+$ cell-injected group and the Flk-1$^+$ cell-sheet group as compared to the control group and the Flk-1$^+$ cell-ECM group on postoperative day 7. The VEGF and bFGF mRNA levels were higher in the Flk-1$^+$ cell-sheet group than in the Flk-1$^+$ cell-injected group (Figure 5B and C). The Flk-1$^+$ cell sheet group also showed a significant decrease in the proportion of TUNEL-positive apoptotic cells in host ischemic muscles as compared with the Flk-1$^+$ cell-injected group and the Flk-1$^+$ cell-ECM group (Figure 5D). In the *in vitro* experiments, treatment with a glutathione (GSH)-depleting agent, L-buthionine-[S,R]-sulfoximine (BSO), increased the ratio of trypan blue positive-dead cells in iPS cell-derived Flk-1$^+$ cells, and this effect was attenuated by MCL labeling (Supplementary figure 4). Collectively, implantation of an iPS cell-derived Flk-1$^+$ cell sheet promoted angiogenesis more effectively than the conventional direct-injection of an Flk-1$^+$ cell suspension.

Finally, we assessed whether or not cell sheets created using Mag-TE elicited a foreign body reaction. The ECM precursor gel sheet created using Mag-TE was placed on the adductor muscles of mice with a C57/BL6 background. Tissue samples were stained with hematoxylin-eosin for evaluation of inflammatory responses. We also assessed the mRNA levels of pro-inflammatory cytokines in muscle tissues after transplantation using real-time PCR. Transplantation of cell sheets created by Mag-TE did not induce the recruitment of neutrophils to muscle (Supplementary figure 5A). In addition, the expression levels of pro-inflammatory cytokines such as IL-6 and MCP-1 were not affected by sheet transplantation (Supplementary figure 5B and C). These results indicated that transplantation of cell sheets created by Mag-TE did not elicit a foreign body reaction.

Discussion

The present study yielded three major findings: (i) We successfully created multi-layered iPS cell-derived Flk-1$^+$ and Flk-1$^-$ cell sheets by combining a new TE modality, termed the Mag-TE system, and the ECM precursor embedding system. (ii) Implantation of iPS cell-derived Flk-1$^+$ cell sheets augmented ischemia-induced angiogenesis. (iii) Implantation of iPS cell-derived Flk-1$^+$ cell sheets increased VEGF and bFGF gene expressions in ischemic muscle *in vivo*.

Recently, some research groups have conducted iPS cell sheet-based TE utilizing monolayer cell sheets harvested from temperature-sensitive culture surfaces[23]. It has been shown that a sheet comprising 3 or more layers, obtained by employing temperature-responsive culture surfaces, suffers central apoptosis or necrosis due to lack of oxygen[23–30]. Previously, we attempted to create iPS cell sheets using only the Mag-TE method. However, this attempt was unsuccessful because central apoptosis was induced in iPS cell sheets due to lack of oxygen. It is noteworthy that the multi-layered sheet created by the combination of Mag-TE and ECM precursor embedding systems led to eventual formation of a "reticular pattern structure". In other words, the combination of Mag-TE and ECM precursor embedding systems resolved the difficulty encountered in creating multi-layered iPS cell sheets by improving cell viability within the sheet. Furthermore, it takes only 24 h to create our multi-layered sheets. These iPS cell-derived Flk-1$^+$ cell sheets, devised employing our novel approach, are extremely viable and convenient. Taken together, these results suggest our new method to be a potentially novel strategy in the field of regenerative medicine using cell sheets.

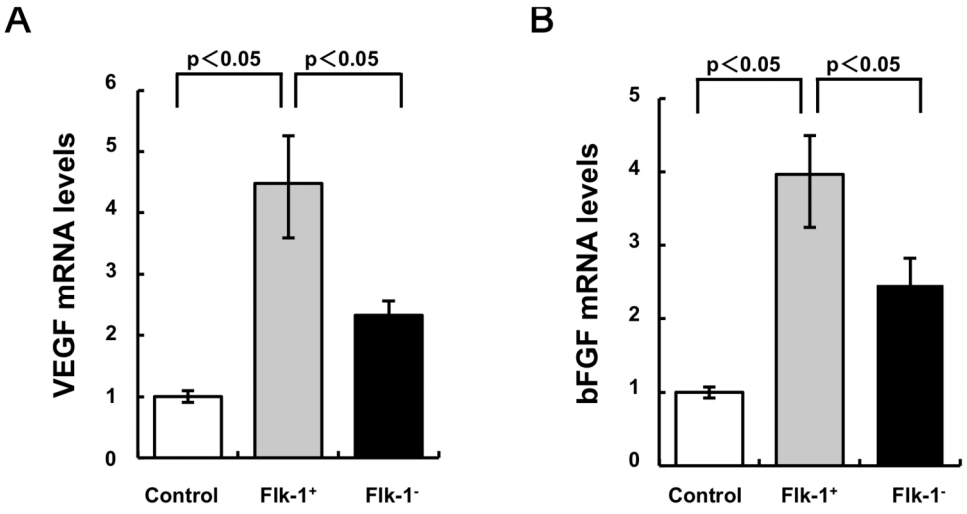

Figure 4 | Implantation of iPS cell-derived Flk-1$^+$ cell sheets stimulated VEGF and bFGF expressions in ischemic tissues. VEGF (A) and bFGF (B) syntheses in ischemic hindlimb muscles on postoperative day 7 were determined by real-time RT-PCR. Results are expressed as VEGF or bFGF mRNA levels relative to GAPDH mRNA levels (n = 4 in each group).

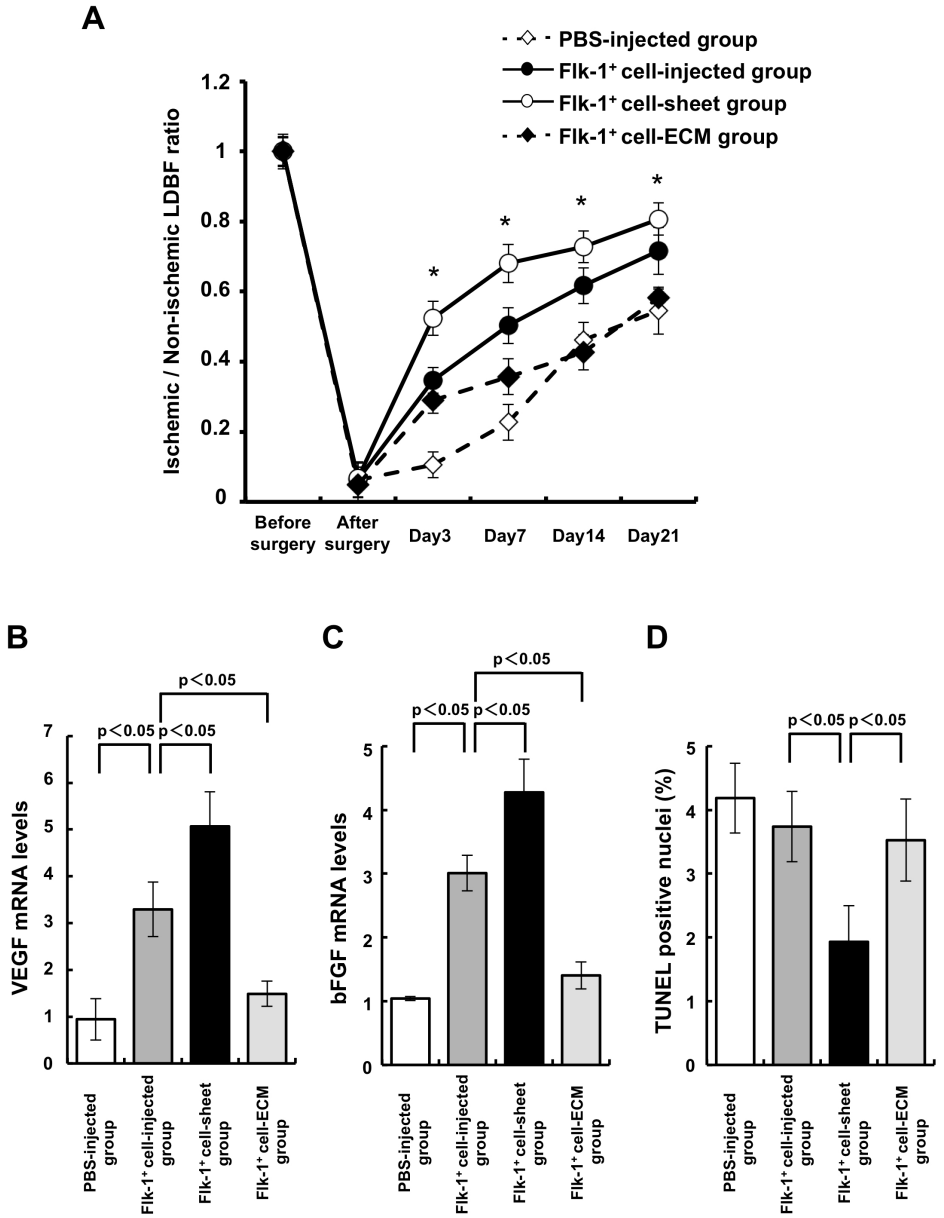

Figure 5 | Implantation of iPS cell-derived Flk-1$^+$ cell sheets promotes angiogenesis more effectively than the conventional direct-injection of a suspension of Flk-1$^+$ cells. (A) Quantitative analysis of the ischemic/normal LDBF ratios in the Flk-1$^+$ cell-sheet, Flk-1$^+$ cell-injected, Flk-1$^+$ cell-ECM and control PBS groups. *$p < 0.05$ vs. Flk-1$^+$ cell-injected group. VEGF (B) and bFGF (C) syntheses in ischemic hindlimb muscles on postoperative day 7 were determined by real-time RT-PCR. Results are expressed as VEGF or bFGF mRNA levels relative to GAPDH mRNA levels. (D) Quantitative analysis of TUNEL positive apoptotic cells in host ischemic tissues (n = 5 in each group).

We have also created iPS cell sheets using only the ECM precursor embedding system, and assessed the effect of this type of sheet on blood flow recovery of ischemic muscle. The sheet created employing only the ECM precursor embedding system had the problem of fluctuating cellular density and did not have a truly sheet-like structure. Furthermore, implantation of iPS cell-derived Flk-1$^+$ cell sheets, created by combining the Mag-TE and ECM precursor embedding systems, promoted angiogenesis more effectively than those obtained with only the latter system. In addition to these results, we have shown that MCL labeling is itself likely to contribute to cell survival via stimulation of peroxidase-like anti-oxidative activities. Thus, having a pre-formed sheet-like structure obtained using the combination of Mag-TE and ECM precursor embedding systems achieves therapeutic benefit as compared to simply mixing the cells with the ECM.

One of the major mechanisms underlying the effects of iPS cell-derived Flk-1$^+$ cell sheet therapy is mediation of angiogenesis via release of angiogenic cytokines such as VEGF and bFGF rather than direct differentiation of transplanted cells into mature endothelial cells[8,31,32]. We previously showed that direct local implantation of mouse iPS cell-derived Flk-1$^+$ cells by conventional needle injections augmented VEGF expression in ischemic tissues[12]. We confirmed that VEGF and bFGF mRNA expressions in ischemic tissues were significantly increased by implantation of iPS cell-derived Flk-1$^+$ cell sheets. Furthermore, VEGF and bFGF levels were higher in the Flk-1$^+$ cell-sheet group than in the Flk-1$^+$ cell-injected group. Thus, the use of multi-layered cell sheets could lead to stable and continuous secretion of angiogenic factors such as VEGF from numerous resident implanted cells, while minimally impacting the implanted tissue. It is reasonable to speculate that iPS cell-derived

Flk-1$^+$ cell sheet implantation promotes angiogenesis more effectively than the conventional Flk-1$^+$ cell suspension direct-injection method.

Several reports have suggested that magnetic nanoparticles may elicit DNA damage in lung epithelial cells and hepatoma cells[33,34]. In contrast, we and other groups have shown Fe_3O_4 nanoparticles themselves to have an intrinsic peroxidase-like activity when magnetic nanoparticle-containing liposomes (MCLs) were co-incubated with various stem cells[35,36]. In cultured human mesenchymal stem cells, MCL-labeling inhibited BSO (the aforementioned GSH-depleting agent)-induced cell death and the expression of the pro-apoptotic protein Bax[36]. We confirmed that treatment with BSO increased the ratio of trypan blue positive-dead cells among iPS cell-derived Flk-1$^+$ cells, and that this effect was attenuated by MCL labeling. Thus, the MCL labeling is itself likely to contribute to stem cell survival via stimulation of peroxidase-like anti-oxidative activity.

In the present study, there was no tumor formation at any point during the observation period in mice transplanted with Flk-1$^+$ cell sheets. However, transplantation of the Flk-1$^+$ cell sheet was associated with significant rates of teratoma formation. In this regard, we used the Flk-1 negative population as Flk-1$^-$ cell sheets, whereas Flk-1 positive and Nanog-negative cells were used as Flk-1$^+$ cell sheets. It is safer to transplant differentiated rather than undifferentiated iPS cells in order to avoid potential teratoma formation[37]. Thus, it is possible that Nanog positive cells included in the Flk-1 negative population can produce teratomas after Flk-1$^-$ cell sheet transplantation. Further long-term experiments are needed to exclude the possibility of tumor formation by cellular contaminants present in small amounts.

Finally, both iPS cell-derived Flk-1$^-$ cells and ECM precursor gel were used as controls. However, a better negative control cell group would be cell sheets containing the parental MEFs, since the FLK1$^-$ cells consist of a highly heterogeneous population which is difficult to characterize.

In conclusion, our iPS cell-derived Flk-1$^+$ cell sheet, created by combining our novel Mag-TE system and the ECM precursor embedding system, was successfully engrafted into ischemic tissues of nude mice and promoted revascularization. Transplantation of iPS cell-derived Flk-1$^+$ cell sheets may become a novel regenerative medicine strategy for ischemic limbs as well as cardiac diseases in the future.

Methods

All protocols were approved by the Institutional Animal Care and Use Committee of Nagoya University School of Medicine. Investigators conducting the follow-up examinations were blinded to the identities of the treated animals.

Reagents. Biotin conjugated anti-mouse Flk-1 antibodies, Allophycocyanin (APC) conjugated anti-mouse Flk-1, were purchased from eBioscience (San Diego, CA, USA). Fluorescein isothiocyanate conjugated anti-mouse CD31 monoclonal antibodies were purchased from BD Pharmingen (San Diego, CA, USA). Monoclonal antibodies for mouse αSMA were purchased from SIGMA-ALDRICH (St Louis, MO, USA).

Cell Culture. Germline competent mouse iPS cell lines, termed "iPS-MEF-Ng-20D-17", which were generated from mouse embryonic fibroblasts by introducing four factors (Oct3/4, Sox2, Klf4 and the c-Myc mutant c-Myc T58A) using retroviral vectors, were provided by Riken Cell Bank with the permission of Dr. S. Yamanaka[9]. In some experiments, another mouse iPS cell line, BM21, generated from dendritic cells of 21-month-old C57/BL6 mice, was used[22]. iPS cells were maintained in Dulbecco's modified Eagle's medium (Invitrogen) containing 10% Knockout Serum Replacement, 1% fetal bovine serum (FBS), nonessential amino acids, 5.5 mmol/L 2-mercaptoethanol, 50 U/mL penicillin and 50 mg/mL streptomycin on feeder layers of mitomycin-C–treated mouse embryonic fibroblast cells stably releasing leukemia inhibitory factor (LIF). Cell differentiation was induced as described previously[10]. In brief, differentiation medium (DM) (α-minimum essential medium supplemented with 10% FBS and 5×10^{-5} mol/L 2-mercaptoethanol) was used for iPS cell differentiation. Flk-1$^+$ mesodermal cells were induced by cultivating iPS cells (plated at 1.7×10^3 cells/cm^2) in DM in the absence of LIF on type IV collagen-coated dishes (ASAHI GLASS CO., LTD, Tokyo, Japan).

Cell separation. Cultured cells were harvested after induction of undifferentiated iPS cells cultivated in DM on type IV collagen-coated dishes. Induced cells were stained with biotin conjugated anti-mouse Flk-1 antibody followed by APC streptavidin secondary antibody. Flk-1$^+$ cells were identified and sorted by fluorescence-activated cell sorting; FACS (BD FACS Aria; Becton Dickinson, Franklin Lakes, NJ, USA). Induced cells were stained with APC conjugated anti-mouse Flk-1 antibody. Stained cells were analyzed employing BD FACS Canto (Becton Dickinson) and FlowJo software (Tree Star, Ashland, OR, USA). Purified Flk-1$^+$ cells were re-plated on type IV collagen-coated dishes with DM in the presence of human $VEGF_{165}$ (WAKO, Osaka, Japan), 8bromo-cAMP (Nacalai Tesque, Kyoto, Japan) and SB-431542 (SIGMA). Four days later, re-plated Flk-1$^+$ cells had differentiated into mature vascular cells. Differentiated cells were assessed by staining with CD31 or α-SMA. In some experiments, Flk-1$^+$ cells with or without MCL labeling (100 pg-magnetite/cell) were treated with 1 mM BSO. After 48 h, cell viability was assessed by trypan blue exclusion.

Construction of cell sheets. iPS cell-derived cell sheets were constructed using the Mag-TE system and the ECM precursor embedding system, in combination. To magnetically label the cells, purified cells were first incubated with MCLs at a concentration of 100 pg-magnetite/cell. After a 2-h incubation, 1×10^6 cells labeled with MCLs were mixed with type I collagen (Cellmatrix Type-I^{TM}, Nitta-gelatin) and matrigel (BD Matrigel^{TM} Basement Membrane Matrix Growth Factor Reduced, BD). These cells were then seeded into a 24-well ultra-low-attachment cell culture plate (Corning, NY, USA). A cylindrical neodymium magnet (magnetic induction, 4000 Gauss) was placed on the reverse side of the ultra-low-attachment plate to provide magnetic force vertical to the plate, and the cells were cultured for an additional 24 h. After this culture, the neodymium magnet on the reverse side of the culture plate was removed. In some experiments, we created iPS cell sheets using only the ECM precursor embedding system.

Mouse model of hindlimb ischemia. Male KSN athymic nude mice or C57BL/6J mice were used for this study. Mice, at age 8 weeks, were subjected to operative unilateral hindlimb ischemia under anesthesia with sodium pentobarbital (50 mg/kg i.p.) as described previously[38,39]. In some experiments, iPS cell-derived Flk-1$^+$ cells with or without MCL labeling (1×10^6 cells/200 μl in PBS) were transplanted into 6 sites in the ischemic limb via a needle injection.

Laser Doppler blood flow analysis. Hindlimb blood flow was measured using a LDBF analyzer (Moor LDI; Moor Instruments, Devon, United Kingdom). Immediately before surgery and on postoperative days 3, 7, 14 and 21, LDBF analyses were performed on legs and feet. Blood flow was displayed as changes in laser frequency using different color pixels. After scanning, stored images were analyzed to quantify blood flow. To avoid data variations due to ambient light and temperature, hindlimb blood flow was expressed as the left (ischemic) to right (non-ischemic) LDBF ratio[38,39].

Immunohistochemical analysis. For histological evaluation, tissue samples were obtained from the ischemic thigh adductor skeletal muscles beneath the cell sheet on postoperative day 21. Frozen tissue sections 6 μm in thickness were prepared from each sample. Tissue sections were stained with hematoxylin and eosin. Capillary density in adductor muscles was analyzed to obtain specific evidence of vascularity at the microcirculatory level. Capillary endothelial cells were identified by immunohistochemical staining with CD31 monoclonal antibody. Fifteen random microscopic fields from three different sections in each tissue block were examined for the presence of capillary endothelial cells. Capillary density was expressed as the number of CD-31-positive features per high power field (×400) and the number of capillaries per muscle fiber[39]. To examine apoptotic cell death in adductor muscles, we performed TUNEL staining using an In Situ Cell Death Detection Kit as previously described (Roche, Mannheim, Germany)[36,40]. DAPI was used for nuclear staining. Ten randomly chosen microscopic fields from four different sections in each tissue block were examined for the presence of TUNEL positive cells.

Reverse Transcription PCR Analysis. Total RNA from adductor muscles was extracted using a FastRNA Pro Green Kit (MP Biomedicals, OH, USA). Reverse transcription was performed with 1 μg of RNA, random primers and MMLV reverse transcriptase (ReverTraAce-α TOYOBO, Osaka, Japan). Quantitative real-time PCR was performed with a LightCyclerT System (Roche Diagnostics, IN, USA) and a QuantiTect SYBR Green PCR kit. Primers: mouse VEGF: sense, 5′-CAGGCTGCT GTAACGATGAA-3′ and antisense, 5′- GCATTCACATCTGCTGTGCT-3′, mouse bFGF: sense, 5′-AGCGGCTCTACTGCAAGAAC-3′ and antisense, 5′-GCCGTC CATCTTCCTTCATA-3′, mouse IL-6: sense, 5′- AGTTGCCTTCTTGGGACTG-3′ and antisense, 5′- TCCACGATTTCCCAGAGAAC-3′, mouse MCP-1: sense, 5′- AGGTCCCTGTCATGCTTCTG-3′ and antisense, 5′- TCTGGACCCATTCCT TCTTG-3′, mouse GAPDH: sense, 5′-AACTTTGGCATTGTGGAAGG-3′ and antisense, 5′-ACACATTGGGGGTAGGAACA-3′.

Statistical Analysis. All analyses were performed using PASW Statistics18 software (SPSS Inc., IL, USA). Student's *t* test was used for comparisons between two groups. One-way ANOVA was employed for comparisons among multiple groups. Repeated-measures ANOVA was used for the blood flow data analyses. $P < 0.05$ was considered significant. All data are presented as means ± SEM.

1. Tateishi-Yuyama, E. *et al.* Therapeutic angiogenesis for patients with limb ischaemia by autologous transplantation of bone-marrow cells: a pilot study and a randomised controlled trial. *Lancet* **360**, 427–435 (2002).

2. Higashi, Y. *et al.* Autologous bone-marrow mononuclear cell implantation improves endothelium-dependent vasodilation in patients with limb ischemia. *Circulation* **109**, 1215–1218 (2004).
3. Amann, B., Luedemann, C., Ratei, R. & Schmidt-Lucke, J. A. Autologous bone marrow cell transplantation increases leg perfusion and reduces amputations in patients with advanced critical limb ischemia due to peripheral artery disease. *Cell Transplant* **18**, 371–380 (2009).
4. Idei, N. *et al.* Autologous bone-marrow mononuclear cell implantation reduces long-term major amputation risk in patients with critical limb ischemia: a comparison of atherosclerotic peripheral arterial disease and Buerger disease. *Circ Cardiovasc Interv* **4**, 15–25 (2011).
5. Assmus, B. *et al.* Transcoronary transplantation of progenitor cells after myocardial infarction. *N Engl J Med* **355**, 1222–1232 (2006).
6. Kajiguchi, M. *et al.* Safety and efficacy of autologous progenitor cell transplantation for therapeutic angiogenesis in patients with critical limb ischemia. *Circ J* **71**, 196–201 (2007).
7. Matoba, S. *et al.* Long-term clinical outcome after intramuscular implantation of bone marrow mononuclear cells (Therapeutic Angiogenesis by Cell Transplantation [TACT] trial) in patients with chronic limb ischemia. *Am Heart J* **156**, 1010–1018 (2008).
8. Heeschen, C. *et al.* Profoundly reduced neovascularization capacity of bone marrow mononuclear cells derived from patients with chronic ischemic heart disease. *Circulation* **109**, 1615–1622 (2004).
9. Takahashi, K. & Yamanaka, S. Induction of pluripotent stem cells from mouse embryonic and adult fibroblast cultures by defined factors. *Cell* **126**, 663–676 (2006).
10. Narazaki, G. *et al.* Directed and systematic differentiation of cardiovascular cells from mouse induced pluripotent stem cells. *Circulation* **118**, 498–506 (2008).
11. Taura, D. *et al.* Induction and isolation of vascular cells from human induced pluripotent stem cells--brief report. *Arterioscler Thromb Vasc Biol* **29**, 1100–1103 (2009).
12. Suzuki, H. *et al.* Therapeutic angiogenesis by transplantation of induced pluripotent stem cell-derived Flk-1 positive cells. *BMC Cell Biol* **11**, 72 (2010).
13. Zhang, M. *et al.* Cardiomyocyte grafting for cardiac repair: graft cell death and anti-death strategies. *J Mol Cell Cardiol* **33**, 907–921 (2001).
14. Müller-Ehmsen, J. *et al.* Survival and development of neonatal rat cardiomyocytes transplanted into adult myocardium. *J Mol Cell Cardiol* **34**, 107–116 (2002).
15. Pittenger, M. F. & Martin, B. J. Mesenchymal stem cells and their potential as cardiac therapeutics. *Circ Res* **95**, 9–20 (2004).
16. Tang, Y. L. *et al.* Improved graft mesenchymal stem cell survival in ischemic heart with a hypoxia-regulated heme oxygenase-1 vector. *J Am Coll Cardiol* **46**, 1339–1350 (2005).
17. Hattori, F. *et al.* Nongenetic method for purifying stem cell-derived cardiomyocytes. *Nat Methods* **7**, 61–66 (2010).
18. Ito, A. *et al.* Construction and harvest of multilayered keratinocyte sheets using magnetite nanoparticles and magnetic force. *Tissue Eng* **10**, 873–880 (2004).
19. Shimizu, K. *et al.* Construction of multi-layered cardiomyocyte sheets using magnetite nanoparticles and magnetic force. *Biotechnol Bioeng* **96**, 803–809 (2007).
20. Ito, A. *et al.* Tissue engineering using magnetite nanoparticles and magnetic force: heterotypic layers of cocultured hepatocytes and endothelial cells. *Tissue Eng* **10**, 833–840 (2004).
21. Ishii, M. *et al.* Enhanced angiogenesis by transplantation of mesenchymal stem cell sheet created by a novel magnetic tissue engineering method. *Arterioscler Thromb Vasc Biol* **31**, 2210–2215 (2011).
22. Suzuki, H. *et al.* Comparative angiogenic activities of induced pluripotent stem cells derived from young and old mice. *PLoS One* **7**, e39562 (2012).
23. Hibino, N. *et al.* Evaluation of the use of an induced puripotent stem cell sheet for the construction of tissue-engineered vascular grafts. *J Thorac Cardiovasc Surg* **143**, 696–703 (2012).
24. Shimizu, T. *et al.* Fabrication of pulsatile cardiac tissue grafts using a novel 3-dimensional cell sheet manipulation technique and temperature-responsive cell culture surfaces. *Circ Res* **90**, e40 (2002).
25. Shimizu, T., Yamato, M., Kikuchi, A. & Okano, T. Cell sheet engineering for myocardial tissue reconstruction. *Biomaterials* **24**, 2309–2316 (2003).
26. Miyagawa, S. *et al.* Tissue cardiomyoplasty using bioengineered contractile cardiomyocyte sheets to repair damaged myocardium: their integration with recipient myocardium. *Transplantation* **80**, 1586–1595 (2005).
27. Memon, I. A. *et al.* Repair of impaired myocardium by means of implantation of engineered autologous myoblast sheets. *J Thorac Cardiovasc Surg* **130**, 1333–1341 (2005).
28. Shimizu, T. *et al.* Polysurgery of cell sheet grafts overcomes diffusion limits to produce thick, vascularized myocardial tissues. *FASEB J* **20**, 708–710 (2006).
29. Matsuura, K. *et al.* Transplantation of cardiac progenitor cells ameliorates cardiac dysfunction after myocardial infarction in mice. *J Clin Invest* **119**, 2204–2217 (2009).
30. Miyahara, Y. *et al.* Monolayered mesenchymal stem cells repair scarred myocardium after myocardial infarction. *Nat Med* **12**, 459–465 (2006).
31. Tse, H. F. *et al.* Paracrine effects of direct intramyocardial implantation of bone marrow derived cells to enhance neovascularization in chronic ischaemic myocardium. *Eur J Heart Fail* **9**, 747–753 (2007).
32. Tateno, K. *et al.* Critical roles of muscle-secreted angiogenic factors in therapeutic neovascularization. *Circ Res* **98**, 1194–1202 (2006).
33. Kai, W., Xiaojun, X., Ximing, P., Zhenqing, H. & Qiqing, Z. Cytotoxic effects and the mechanism of three types of magnetic nanoparticles on human hepatoma BEL-7402 cells. *Nanoscale research letters* **6**, 480 (2011).
34. Konczol, M. *et al.* Cytotoxicity and genotoxicity of size-fractionated iron oxide (magnetite) in A549 human lung epithelial cells: role of ROS, JNK, and NF-kappaB. *Chemical research in toxicology* **24**, 1460–1475 (2011).
35. Gao, L. *et al.* Intrinsic peroxidase-like activity of ferromagnetic nanoparticles. *Nature nanotechnology* **2**, 577–583 (2007).
36. Ishii, M. *et al.* Enhanced angiogenesis by transplantation of mesenchymal stem cell sheet created by a novel magnetic tissue engineering method. *Arterioscler Thromb Vasc Biol* **31**, 2210–2215 (2011).
37. Okita, K., Nagata, N. & Yamanaka, S. Immunogenicity of induced pluripotent stem cells. *Circ Res* **109**, 720–721 (2011).
38. Murohara, T. *et al.* Nitric oxide synthase modulates angiogenesis in response to tissue ischemia. *J Clin Invest* **101**, 2567–2578 (1998).
39. Shibata, R. *et al.* Adiponectin stimulates angiogenesis in response to tissue ischemia through stimulation of amp-activated protein kinase signaling. *J Biol Chem* **279**, 28670–28674 (2004).
40. Maruyama, S. *et al.* Adiponectin ameliorates doxorubicin-induced cardiotoxicity through Akt protein-dependent mechanism. *J Biol Chem* **286**, 32790–32800 (2011).

Acknowledgments

We are grateful to Yoko Inoue for technical assistance. This study was supported by grants (No. 21590951 to S.S. and No. 20249045 to T.M.) from the Ministry of Education, Culture, Sports, Science and Technology of Japan; and a grant for advancement of translational research from the Japanese Circulation Society to T.M.

Author contributions

T.K., R.S., M.I., H.S., T.Y., Y. K., Y. Y., J. Y. and T.M. designed and carried out the studies. T.H., N.N., S.I., Y. N., T. T., N. O., H. H. and K.I. analyzed the data. T.M. and R.S. wrote the paper.

Additional information

Supplementary information accompanies this paper at http://www.nature.com/scientificreports

Competing financial interests: The authors declare no competing financial interests.

How to cite this article: Kito, T. *et al.* iPS cell sheets created by a novel magnetite tissue engineering method for reparative angiogenesis. *Sci. Rep.* **3**, 1418; DOI:10.1038/srep01418 (2013).